

Article

Carbohydrate Dynamics in Maize Leaves and Developing Ears in Response to Nitrogen Application

Peng Ning^{1,2} , Yunfeng Peng^{2,3} and Felix B. Fritsch^{2,*}

¹ College of Natural Resources and Environment, Northwest A&F University, Yangling 712100, Shaanxi, China; ningp@nwfau.edu.cn

² Division of Plant Sciences 1-31 Agriculture Building, University of Missouri, Columbia, MO 65211, USA; pengyf@ibcas.ac.cn

³ Key Laboratory of Vegetation and Environmental Change, Institute of Botany, The Chinese Academy of Sciences, Beijing 100093, China

* Correspondence: fritschf@missouri.edu; Tel.: +1-573-882-3023

Received: 4 November 2018; Accepted: 12 December 2018; Published: 15 December 2018



Abstract: Maize grain yield is considered to be highly associated with ear and leaf carbohydrate dynamics during the critical period bracketing silking and during the fast grain filling phase. However, a full understanding of how differences in N availability/plant N status influence carbohydrate dynamics and processes underlying yield formation remains elusive. Two field experiments were conducted to examine maize ear development, grain yield and the dynamics of carbohydrates in maize ear leaves and developing ears in response to differences in N availability. Increasing N availability stimulated ear growth during the critical two weeks bracketing silking and during the fast grain-filling phase, consequently resulting in greater maize grain yield. In ear leaves, sucrose and starch concentrations exhibited an obvious diurnal pattern at both silking and 20 days after silking, and N fertilization led to more carbon flux to sucrose biosynthesis than to starch accumulation. The elevated transcript abundance of key genes involved in starch biosynthesis and maltose export, as well as the sugar transporters (SWEETs) important for phloem loading, indicated greater starch turnover and sucrose export from leaves under N-fertilized conditions. In developing ears, N fertilization likely enhanced the cleavage of sucrose to glucose and fructose in the cob prior to and at silking and the synthesis from glucose and fructose to sucrose in the kernels after silking, and thus increasing kernel setting and filling. At the end, we propose a source-sink carbon partitioning framework to illustrate how N application influences carbon assimilation in leaves, transport, and conversions in developing reproductive tissues, ultimately leading to greater yield.

Keywords: grain yield; nitrogen; nonstructural soluble carbohydrate (NSC); starch; sucrose; *Zea mays* L.

1. Introduction

Maize (*Zea mays* L.) is one of the world major crops and an important food source for the growing population [1]. Generally, maize yields are strongly correlated with amounts of nitrogen (N) fertilizer applied to the crop. The grain yield of maize is considered to be greatly dependent on ear growth during the critical period bracketing silking [2,3], that is, around 1 week before to 2 weeks after silking [4–6]. At this stage, carbon assimilation in leaves, photoassimilate (mainly sucrose) transport in the phloem, and carbohydrate interconversion and transport between the maternal tissues and developing kernels are important steps which determine grain filling and yield formation [7,8]. Therefore, a better understanding of N effects on carbohydrate dynamics in leaves and the developing ear is pivotal to improve maize N use efficiency as well as yields under N-deficient conditions.

Over the past decades, numerous studies have been conducted to examine the effects of N supply on leaf growth and photosynthetic capacity [9–12], leaf carbohydrate concentrations [13–15], sucrose loading and transport in the phloem [8], and ear growth and carbohydrate dynamics [13–16], and how these factors influence yield and yield components. For instance, increased grain yield in response to N application was associated with greater leaf area [9–11], ear dry weight (DW) [13–15], and developing kernel number per ear [17]. Enhanced maize yield with N fertilization has been positively associated with increased leaf total and soluble protein concentrations [9,14,18,19], as well as kernel soluble protein [16,20] and starch concentrations [16,21], but yield improvement was negatively related to increasing soluble carbohydrate concentrations in the developing kernels [16,21]. Although these studies have advanced our knowledge of the mechanism underlying yield increases in maize in response to N applications, questions remain about how N status influences the carbohydrate dynamics in leaves, sucrose transport from source to developing sink and carbohydrate conversion in the maternal tissues and growing kernels, and their correlations with yield production.

To address some of these questions, we conducted two field experiments to examine carbohydrate dynamics at early stages of ear development and the fast grain filling phase in response to three N application levels (zero-N, medium and high N levels). In Experiment I, we measured ear growth and nonstructural soluble carbohydrate (NSC) dynamics in developing ears from 10 days before silking (DBS) to physiological maturity. In Experiment II, we examined the diurnal dynamics of the NSC in maize ear-leaves at silking and 20 days after silking (DAS), and the associated expression of genes involved in sucrose export and starch turnover. Based on these results, we present a framework of how N application affects leaf carbohydrate assimilation, sugar export from leaves, and carbohydrate conversion and transport in maternal tissues and developing kernels, ultimately leading to enhanced grain yield.

2. Materials and Methods

2.1. Site Description

Field experiments were performed at the University of Missouri Bradford Research Center, Columbia, MO, USA (38°53' N; 92°12' W) in 2010–2011 and 2015 on a Mexico silt loam (Fine, smectitic, mesic Aeric Vertic Epiaqualf) soil. Experiments in the three years were performed in different field plots. The soil chemical properties in the three years were as follows: pH 6.7, 6.6 and 6.5, organic matter 21, 28 and 31 g kg⁻¹, total-N 1.3 g kg⁻¹ (2010) and 1.6 g kg⁻¹ (2011), mineral N 12 mg kg⁻¹ (2015), Bray-I P 11.5, 14.5 and 6.4 mg kg⁻¹, NH₄OAc extractable K 124, 93 and 78 mg kg⁻¹, respectively. Precipitation during the maize growing season in May, June, July, August and September was 108, 84, 204, 105 and 176 mm in 2010, 136, 83, 59, 61 and 46 mm in 2011, and 140, 129, 204, 106 and 21 mm in 2015, respectively.

Prior to sowing, fields were disked to approximately 0.15 m depth, followed by a single pass with a harrow. Maize hybrid 'Pioneer 32D79' was selected for the study and was sown in rows 0.76 m apart on 25 May 2010, 9 May 2011, and 8 May 2015 to achieve a stand density of 78,000, 72,000, and 78,000 plants ha⁻¹, respectively. A randomized complete block design with four replications was used each year. Weeds were controlled by pre-emergence herbicide application (Atrazine plus S-metolachlor) followed by manually hoeing as needed. Other aspects specific to each of the two experiments are described below.

2.2. Experiment I

Phosphorus and K fertilizer was applied before sowing in 2010 (105 kg ha⁻¹ P₂O₅ and 105 kg ha⁻¹ K₂O) and in 2011 (85 kg ha⁻¹ P₂O₅ and 110 kg ha⁻¹ K₂O). Three N treatments were imposed in 2010 and 2011, i.e., (i) N0, 0 kg N ha⁻¹ as control; (ii) N150, 150 kg N ha⁻¹ applied at planting (N150); and (iii) N300, 150 kg N ha⁻¹ applied at planting, 75 kg N ha⁻¹ applied at V6 (6th leaf fully expanded), and 75 kg N ha⁻¹ applied at V10 (10th leaf fully expanded). Nitrogen was broadcast applied as urea

with an over-the-shoulder broadcast spreader. Individual plots were 9.14 m long and 6.1 m wide in both years.

Developing ears were sampled at 10 and 6 days before silking (DBS), silking, 8 days after silking (DAS) and 63 DAS (R6) in 2010, and 6 DBS, silking, 8, 18, and 57 DAS (R6) in 2011. All plant samplings were performed between 11:00 AM and 1:00 PM. At each sampling, whole ears and ear leaves of eight consecutive plants in a row were removed from each plot and four of them were immediately flash-frozen in liquid N and stored at $-80\text{ }^{\circ}\text{C}$. Ear DW was determined based on the remaining four ears. Ears were separated into cobs and kernels (after silking). Prior to carbohydrate analyses, frozen samples were lyophilized and ground with a coffee grinder and mortar and pestle to obtain a fine powder for carbohydrate assay.

The NSC (glucose, fructose, sucrose) and starch concentrations were assayed as previously described [14,15,22]. Briefly, approximately 30 mg freeze-dried and ground tissue was extracted three times with 1 ml 80% EtOH at $80\text{ }^{\circ}\text{C}$ in a water bath for 15 min. The three supernatants were combined in a test tube and brought to a final volume of 10 ml with 80% (v/v) EtOH. A clear aliquot of 25 μL of supernatant was mixed with 250 μL glucose assay kit (Sigma G3293, Sigma-Aldrich, St. Louis, MO, USA) (a mixture of adenosine tri-phosphate, oxidized nicotinamide adenine dinucleotide, hexokinase, and glucose-6P dehydrogenase), and incubated for 15 min at $30\text{ }^{\circ}\text{C}$, and absorbance at 340 nm was read with a spectrophotometer (GENESYS 10 UV, Thermo Electron Corporation, Madison, WI, USA) to quantify glucose. Fructose was quantified by adding phosphoglucose isomerase (Sigma P9544) to the above aliquots, and determining the amount of glucose released. Finally, invertase (Sigma I4504) was added to obtain the combined concentration of glucose + fructose + sucrose. The pellet remaining after the above extraction was used to determine starch by enzymatic hydrolysis and subsequent quantification of the amount of glucose released [14,15,22]. Alpha-amylase (Sigma-Aldrich, A3403, Sigma-Aldrich, St. Louis, MO, USA) and amyloglucosidase (Sigma-Aldrich, A3042, Sigma-Aldrich, St. Louis, MO, USA) were used to hydrolyze the pellets. The supernatant from enzymatic hydrolysate was assayed for glucose as described above, and starch was calculated from the glucose concentration in the tissue residue.

Maize grain yield was determined each year by hand-harvesting and weighing ears from the central 9.12 m^2 of each plot at physiological maturity. Six randomly selected ears from each plot were shelled and moisture content and kernel percentage were determined. Grain yield per plot was estimated based on kernel percentage and expressed at 15.5% moisture content.

2.3. Experiment II

In 2015, three N levels were included as follows: (i) N0, no N fertilizer as control; (ii) N200, 200 kg N ha^{-1} split equally at emergence and V8 stages (because yield increase in response to the N150 treatments in Experiment I were modest, 200 kg N ha^{-1} was applied instead in 2015); and (iii) N300, 200 kg N applied as described for the N200 treatment, and an additional 100 kg N ha^{-1} applied one week before silking. Each plot consisted of eight 6.1 m long rows, and N was applied manually in the form of urea. Ear leaves from three plants were sampled every 4 h starting at 08.00 h at silking and 20 DAS. The middle ($\sim 10\text{ cm}$) of the leaf blade was dissected to remove the midrib, and the leaf blade tissues from the two sides of the midrib were separated into two groups and immediately immersed into liquid N_2 . One part was stored at $-80\text{ }^{\circ}\text{C}$ and destined for gene expression analysis, and the other one was lyophilized for carbohydrate analysis.

The freeze-dried ear leaves were ground using a coffee grinder and further processed with a Geno/Grinder 2010 (SPEX SamplePrep, Metuchen, NJ, USA). Sugars (glucose, fructose, and sucrose) were extracted and starch solubilized and converted to glucose as described for Experiment I, but quantified by HPLC (Shimadzu Corp., Kyoto, Japan) with a refractive index detector (Model RID-10A) as previously described [8].

Ear leaf samples from the collections at 12:00 at silking and 20 DAS were selected to investigate the expression pattern of genes involved in sucrose and starch metabolism as described previously [8].

Briefly, frozen leaves were ground in liquid N₂, and total RNA was extracted using a RNeasy Plant Mini kit (QIAGEN, Hilden, Germany). Reverse transcription was performed according to the manufacturer's instructions. Quantitative real-time PCR was conducted with β -Tubulin as a reference gene [23] on an ABI 7500 real-time PCR system with universal cycling conditions (95 °C for 2 min, 40 cycles of 95 °C for 15 s, and 60 °C for 1 min) following the manufacturer's instructions. Primers were designed as follows: *Tpt* (forward, 5'-GGA GAA AAG GAA AAA GAG CGC AT-3'; reverse, 5'-ACG ATG TTG TTG TTG TGT CCC-3'); *Agpsl1* (forward, 5'-TGG GAC AGT TAT ATG AAG CGG A-3'; reverse, 5'-TCC ATG ATC TCC AGC ACA CTG-3'); *Agpll1* (forward, 5'-TCC TAA ACC TTC TAA GAT GGC G-3'; reverse, 5'-AAA CTG AAC CTT GGA GGC TGT-3'); *Ss1* (forward, 5'-GCT ATT GGC TCC ATT GCT CC-3'; reverse, 5'-TTC AAA ACT GTC GTT CGG CT-3'); *Bmy3* (forward, 5'-CCC ATG AGG ACG ACC TGC CA-3'; reverse, 5'-TTT ATC ACC CGC CCG TTT ATT TTG-3'); *Mex1-like* (forward, 5'-GGT TGG ACA GCC ACA CTT CT-3'; reverse, 5'-TGC AGA ACC AGT GAA CCA CA-3'); *Sps1* (forward, 5'-CGT TCC TCA TCA AAG ACC CCC-3'; reverse, 5'-ACG GAA AGA TAC CTG AGT GCC T-3'); *Sus2* (forward, 5'-CCA ACC GCA GTA GTA ATG GC-3'; reverse, 5'-CGG CTT GCC AGC AAA GAA AT-3'); *Sweet13a* (forward, 5'-CTG GGC GTT TGC TTT CG-3'; reverse, 5'-ACT TGC TCT TGT AGA TGC GGT A-3'); *Sweet13b* (forward, 5'-TGC GTA CTG CGT AGT TCC AT-3'; reverse, 5'-GGA GAT GAC GTT GCC TAG GAG-3'); *Sweet13c* (forward, 5'-CAA GAG TTT GAG ACA GCA GAG G-3'; reverse, 5'-CCA GGA AGG TCA TGA AGG AG-3'); *Sut1* (forward, 5'-GGC ACA AGT GGT TTC CGT TC-3'; reverse, 5'-TTT GCC TTT GTG GGG AGG TT-3'); *Sus1* (forward, 5'-CGT ACA CCG AGT CGC ACA AGA G-3'; reverse, 5'-TCC ACC AGC CCA GTC AAG TTC T-3'); β -Tubulin (forward, 5'-CTA CCT CAC GGC ATC TGC TAT GT-3'; reverse, 5'-GTC ACA CAC ACT CGA CTT CAC G-3'). Relative expression values were calculated according to the Pfaffl method [24], and expressed as ratios relative to values of normal N supply (N₂₀₀) at time 00:00 h at silking as shown in [8].

2.4. Statistical Analysis

Analysis of variance was employed to examine N treatment effects and treatment means were compared based on least significant difference (LSD) at the 0.05 level of probability. The ANOVA of repeated measurements presented in Figure 2 and Pearson correlations presented in Figure 5 were performed in R. For gene expression in Figure 3, the effects of N treatment and stage (and their interaction) were analyzed with the MIXED procedure in SAS (SAS Institute Inc., Cary, NC, USA). The stage and N treatment factors were considered as fixed and replication as random factors.

3. Results

3.1. Dry Matter Accumulation in Developing Ear (or Kernels) and Final Grain Yield

To provide context for the NCS and gene expression data, grain yield data are presented in Figure 1 (adapted from [8] and [13]). Briefly, compared to the N0 and N150 treatments, the final grain yield of the N300 treatment was increased by 2.1–4.3 fold in 2010 and by 1.2–2.0 fold in 2011, respectively, and significant differences were detected between N0 and N150 in 2010 (Figure 1). Similarly, in 2015, 1.3–1.8 fold increase of grain yield in N200 and N300 treatments was observed in comparison with N0. A 19.3% lower yield was observed in N300 relative to N200 in 2015.

In agreement with the grain yield, N application resulted in greater ear dry matter accumulation from pre-silking to maturity (Table 1). Significant N treatment effects on ear dry weight were observed at –6, 0, and 8 DAS. Particularly during the fast grain filling phase (i.e., from 18 to 57 DAS), dry matter accumulation rate in developing ears was much greater in N300 treatment than N0 and N150 (1.76 vs. 0.57–0.98 g plant⁻¹ day⁻¹) in 2011. The accumulation rate under 200 and 300 kg N ha⁻¹ was also markedly higher than that in the N0 control (3.13–3.86 vs. 1.82 g plant⁻¹ day⁻¹) from 20 to 51 DAS in 2015. Compared to normal N supply (N200), the N300 treatment had 17–18% lower ear dry weight at 20 and 51 DAS in 2015.

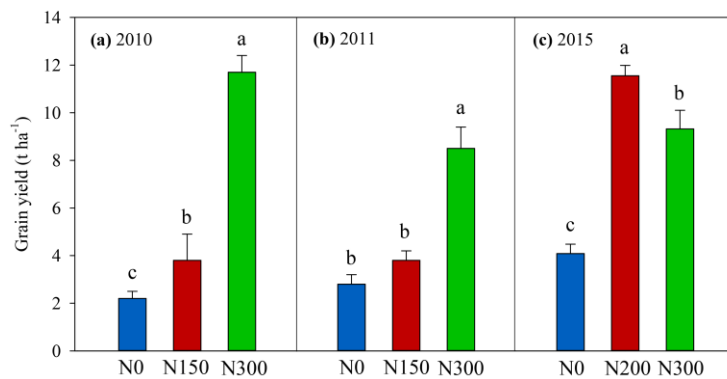


Figure 1. Maize grain yield in response to different nitrogen treatments in 2010 (a), 2011 (b), and 2015 (c) (adapted from [8] and [13]). N0, N150, N200 and N300 represent N treatments that received a total of either 0, 150, 200, or 300 kg N ha⁻¹. Nitrogen was applied as single application (N150) or as split applications (N200, N300). Vertical bars represent the standard error of four replications. Different letters above column indicate significant differences between nitrogen levels by LSD test ($p < 0.05$).

Table 1. Ear dry weight in response to N treatment in 2010, 2011, and 2015. N0, N150, N200, and N300 represent N treatments that received a total of either 0, 150, 200, or 300 kg N ha⁻¹ in the form of single or split fertilizer applications.

| Year | Treatment | Days after Silking | | | | | | |
|------|-----------|--------------------|--------------|--------------|--------------|----------------|---------------|--|
| | | -10 | -6 | 0 | 8 | 63 | | |
| 2010 | N0 | n.d. | 0.1 ± 0.0 b | 1.6 ± 0.4 b | 4.6 ± 0.4 b | - | 37.7 ± 3.9 b | |
| | N150 | 0.1 ± 0.06 b | 0.4 ± 0.2 ab | 3.0 ± 1.6 b | 8.9 ± 2.5 b | - | 56.2 ± 8.2 b | |
| | N300 | 0.21 ± 0.08 a | 1.3 ± 0.4 a | 11.6 ± 2.7 a | 38.0 ± 4.4 a | - | 175.4 ± 5.5 a | |
| 2011 | | | -6 | 0 | 8 | 18 | 57 | |
| | N0 | - | 0.6 ± 0.0 b | 1.1 ± 0.0 b | 4.9 ± 0.9 c | 7.9 ± 1.4 c | 46.2 ± 6.0 b | |
| | N150 | - | 0.9 ± 0.1 b | 2.2 ± 0.4 b | 13.4 ± 1.3 b | 34.4 ± 2.5 b | 56.7 ± 11.0 b | |
| N300 | - | 1.5 ± 0.2 a | 5.1 ± 0.7 a | 35.4 ± 2.4 a | 84.2 ± 8.9 a | 152.9 ± 6.3 a | | |
| 2015 | | | | 0 | | 20 | 51 | |
| | N0 | - | - | 0.9 ± 0.1 b | - | 13.4 ± 1.8 c | 70.0 ± 6.2 c | |
| | N200 | - | - | 2.2 ± 0.6 a | - | 71.3 ± 2.9 a | 191.0 ± 7.2 a | |
| N300 | - | - | 2.1 ± 0.5 a | - | 59.2 ± 6.4 b | 156.1 ± 13.0 b | | |

N0, N150, N200 and N300 represent N treatments that received a total of either 0, 150, 200, or 300 kg N ha⁻¹. Nitrogen was applied as single application (N150) or as split applications (N200, N300). Values indicate mean ± standard error ($n = 4$); Different letters within column within each stage and year indicate significant differences between nitrogen level by LSD test ($p < 0.05$). Unit: g per ear.

3.2. Diurnal Changes of Carbohydrate in Ear Leaves

Pronounced diurnal pattern were observed for sucrose and starch concentrations in ear leaves at both silking and 20 DAS, while glucose and fructose concentrations changed to a lesser extent or did not change significantly during the 24-h periods (Figure 2). Sucrose levels reached the peak at 12:00 to 16:00 and then decreased, while starch accumulated over the course of the day to reach a maximum at 20:00, and was degraded during the night (Figure 2e–h).

Concentrations of all four non-structural carbohydrates were highly responsive to N availability ($p < 0.001$; Figure 2). Nitrogen deficiency (N0) caused lower leaf concentrations of glucose, fructose, and sucrose compared to N fertilized treatments, with particularly strong effects observed for glucose (0 and 20 DAS) and for fructose at 20 DAS. In contrasting to the soluble sugars, starch accumulation was much greater in the N-deficient leaves than in those from N200 and N300 treatments, implying preferential allocation of photoassimilates to starch than to sugars under N starvation.

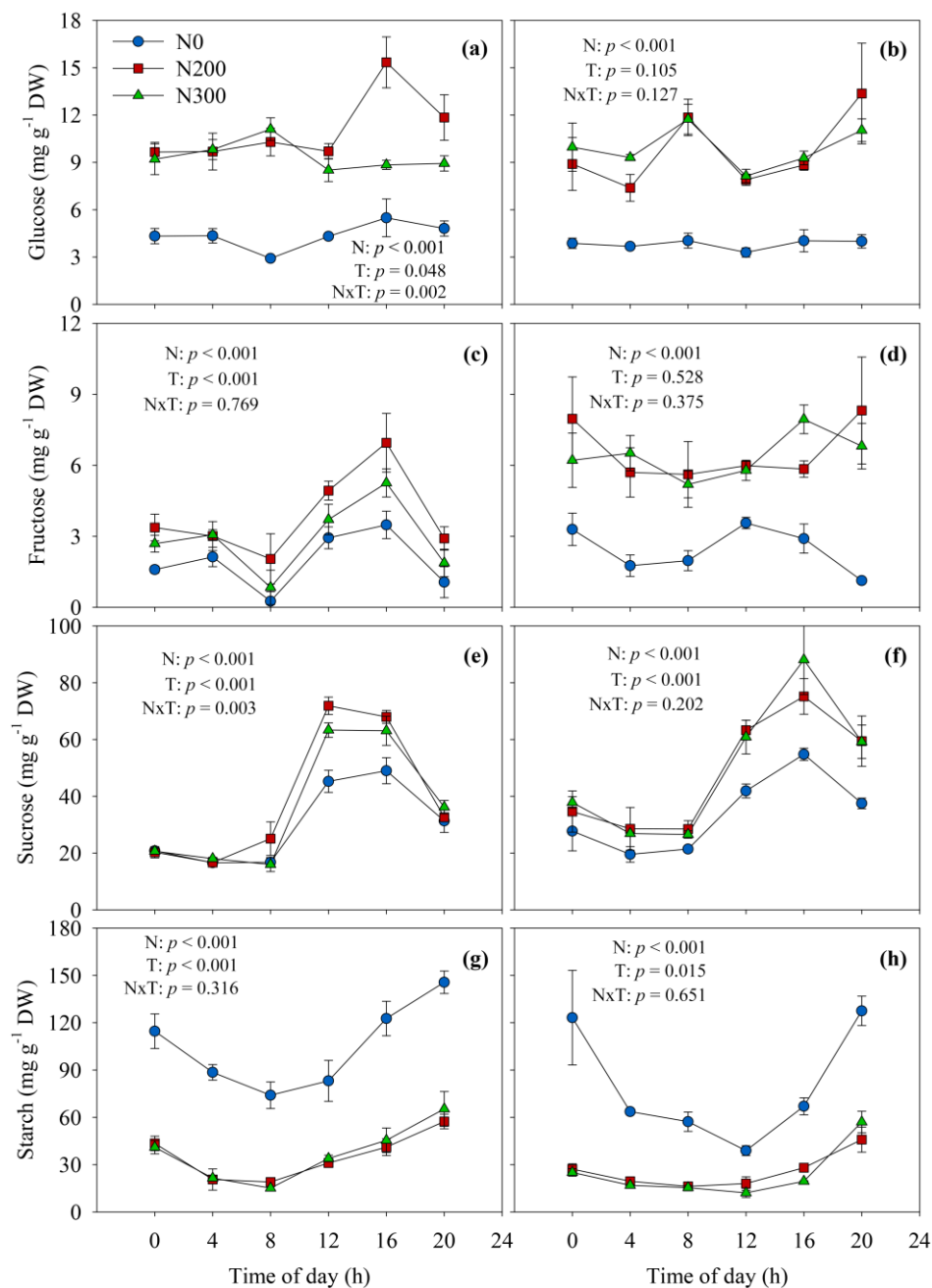


Figure 2. Diurnal dynamics of glucose, fructose, sucrose and starch concentrations in ear leaf at silking (a,c,e,g) and 20 days after silking (b,d,f,h) in 2015. Vertical bars represent the standard error of four replications. N0, N200, and N300 represent N treatments that received a total of either 0, 200, or 300 kg N ha⁻¹ applied as split applications. N, N treatment; T, timepoint.

3.3. Relative Transcript Abundance of Genes Involved in Sucrose and Starch Metabolism in the Ear Leaf

Significant impacts of N availability on relative transcript abundance pattern were observed for all genes at silking or at 20 DAS or at both stages, except for *ZmSus2* (Figure 3). The transcript abundance of the phosphate/triose-phosphate translocator (*ZmTpt*) gene was lower in the N0 leaves than in the N200 and N300 leaves at both 0 and 20 DAS (Figure 3a), hinting that greater starch concentrations could in part be a result of reduced triose-phosphate export from the chloroplast. In agreement with the lower sucrose levels in N-deficient leaves, the relative transcript abundance of sucrose-phosphate synthase (*ZmSps1*) in N0 leaves was suppressed when compared to the N-fertilized treatments (Figure 3b). In contrast, the relative abundance of sucrose synthase (*ZmSus2*) transcripts was not significantly

affected by N treatment (Figure 3c). Of the three *Sweet13* genes (responsible for sucrose export to apoplast), the expression levels of *Sweet13a* and *Sweet13b* were elevated in N-fertilized treatments at 20 DAS and relative transcript abundance of *Sweet13c* was higher in N300 than N0 at both silking and 20 DAS (Figure 3d–f). Relative transcript abundance of the sucrose transporter (*ZmSut1*) responsible for sucrose loading into the phloem increased with increasing N availability at silking, but the differences between N treatments were not different at 20 DAS (Figure 3g).

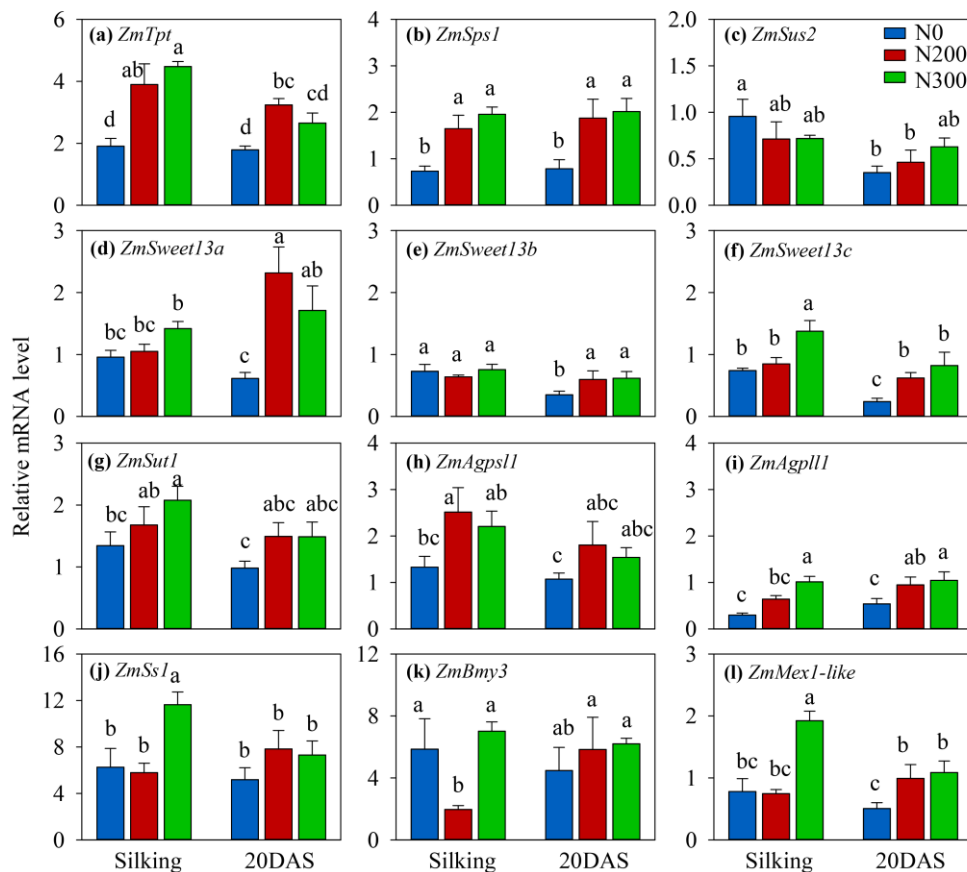


Figure 3. Relative transcript abundance of genes involved in the sucrose and starch metabolism in maize ear leaves sampled at 12:00 h at silking and 20 days after silking (DAS) in 2015. (a) *ZmTpt*, triose-phosphate translocator; (b) *ZmSps1*, sucrose-phosphate synthase1; (c) *ZmSus1*, sucrose synthase; (d–f) *ZmSweet13*, sugars will be eventually exported transporter 13; (g) *ZmSut1*, sucrose transporter1; (h) *ZmAgps1l*, ADP glucose pyrophosphorylase small subunit leaf1; (i) *ZmAgpl1l*, ADP glucose pyrophosphorylase large subunit leaf1; (j) *ZmSs1a*, starch synthase1; (k) *ZmBmy3*, beta-amylase3; (l) *ZmMex1-like*, maltose exporter1-like; Vertical bars represent the standard error of four replicates. Different letters above column indicate significant differences between treatments across nitrogen level and stage by LSD test ($p < 0.05$). N0, N200, and N300 represent N treatments that received a total of either 0, 200, or 300 kg N ha⁻¹ applied as split applications. Adapted from [8].

Of the genes encoding enzymes of starch biosynthesis, significant treatment effects were observed between N0 and N200 at silking for *ZmAgps1l* (Figure 3h). Additionally, the relative transcript abundance of *ZmAgpl1l* increased significantly in N-fertilized treatments at both silking and 20 DAS, while that of *ZmSs1* was significantly higher in the N300 compared to the N0 treatment at silking but not at 20 DAS (Figure 3i,j). Relative transcript level abundance of beta-amylase (*ZmBmy3*) exhibited an inconsistent response to N treatment at silking and did not differ at 20 DAS (Figure 3k). In contrast, the relative RNA levels of the maltose exporter gene (*ZmMex1-like*) were greater in the N300 than the N0 treatment at both silking and 20 DAS (Figure 3l).

3.4. NSC Dynamics in Developing Ears and Kernels

Over the course of ear development, the glucose, fructose, sucrose and starch concentration trends were consistent across N treatments and years (Figure 4). While glucose and fructose concentrations increased (Figure 4a–d), the concentrations of sucrose and starch decreased as the developing ear approached silking (Figure 4e–f). However, while glucose, fructose and sucrose concentrations were greater, starch concentrations were lower in kernels sampled 8 DAS than in mature kernels. Glucose and fructose concentrations in developing kernels decreased dramatically from 8 DAS to 18 DAS, and coincided with a steep increase in starch concentration during the same time period. Significantly negative relationships were observed between the hexoses and sucrose or starch (Figure 5b,c).

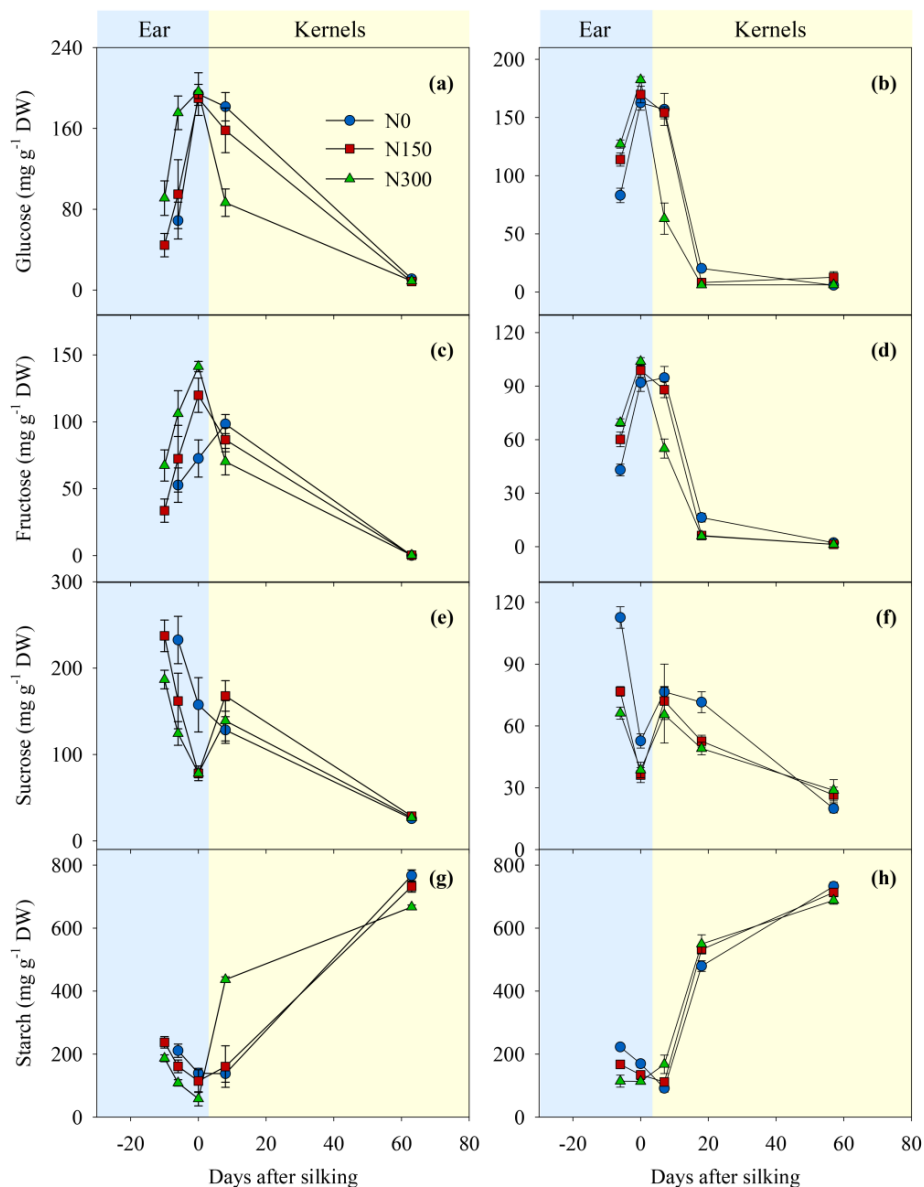


Figure 4. Temporal dynamics of glucose, fructose, sucrose and starch concentrations in the developing ear and kernels in 2010 (a,c,e,g) and 2011 (b,d,f,h). Day 0 indicates silking. Vertical bars represent the standard error of four replicates. Please note that carbohydrate concentrations were measured in the developing ears before and at silking, and in the kernels after silking. N0, N150, and N300 represent N treatments that received a total of either 0, 150, or 300 kg N ha⁻¹, with fertilizer in the N300 treatment applied as split application.

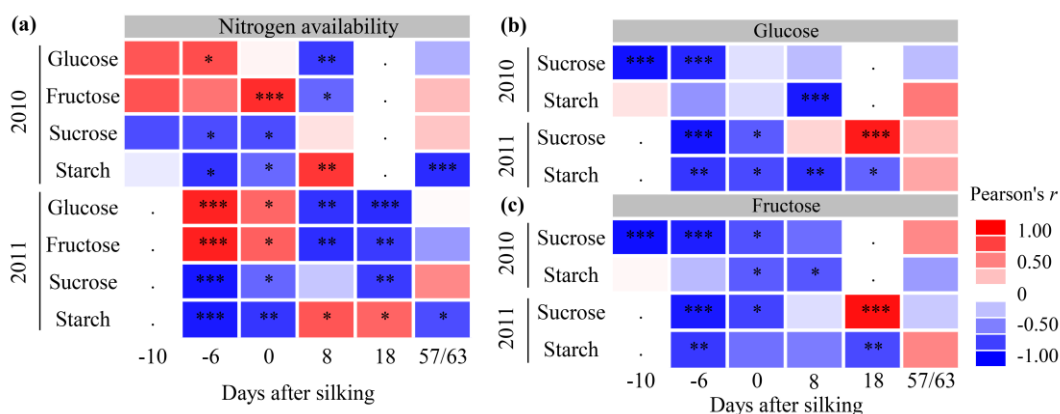


Figure 5. Pearson correlation coefficients between soil N availability and carbohydrate (a), between glucose and sucrose or starch (b), and between fructose and sucrose or starch (c) in developing ear in 2010 and 2011. Dots = not measured. *, $p < 0.05$; **, $p < 0.01$; ***, $p < 0.001$.

Prior to silking, the responses of glucose and fructose concentrations in developing ears to N supply were opposite to those of sucrose and starch. That is, while sucrose and starch concentrations in developing ears decreased with increasing N supply, glucose and fructose concentrations increased with additional N (all $p < 0.05$; Figure 4), which were consistent with the positive response to N supply (Figure 5a). However, in the growing kernels at 8 DAS, glucose and fructose concentrations in the N300 treatments were lower than in the N0 and N150 treatments (both $p < 0.05$). These results reveal a tendency towards an inverse relationship among N treatments and the concentrations of glucose and fructose when compared to pre-silking dynamics. Few differences in sucrose concentrations of the developing and mature kernels were found among N treatments in either year. In 2010, starch concentrations in kernels at 8 DAS were greater in the N300 treatment than the N0 and the N150 treatments, but at maturity, kernel starch concentration were lowest in N300, intermediate in N150, and highest in N0 ($p < 0.05$). In 2011, N fertilized treatments also had greater kernel starch concentrations in developing kernels ($p < 0.05$), and consistent with 2010, kernel starch concentration decreased with increasing N availability at the final harvest (N300 < N150 < N0; $p < 0.05$). In both years, kernel starch concentration at maturity was negatively correlated with N availability (Figure 5a).

4. Discussion

4.1. Nitrogen Application Increases Sugar Biosynthesis and Export from Leaves

Maize grain yield greatly depends on post-silking carbon assimilation in source leaves and allocation to developing ears [25–27]. It has been well documented that N starvation can dramatically suppress carbohydrate biosynthesis through leaf area development and photosynthesis [9,11,12]. At the same time, under N deficiency, leaves accumulate large amounts of carbohydrate as starch in the bundle sheath cells, at the expense of sugar export for growth [8,14,15,28,29]. Therefore, it is crucial to investigate the diurnal pattern of sugar and starch in leaves in response to N availability, particularly at the early and fast grain filling phase.

Of the four types of carbohydrate examined in this study, ear leaf glucose and fructose exhibited relatively weaker diurnal pattern, and largely much lower concentrations, than sucrose and starch at both silking and 20 DAS (Figure 2a–f), which was in agreement with a previous report [14]. The maximum sucrose concentration in ear leaves during the diurnal cycle occurred about 12:00 h to 16:00 h while starch accumulated almost linearly from morning until 20:00 h, regardless of N treatment (Figure 2e–h). The low levels and weak diurnal patterns in glucose and fructose are consistent with rapid assimilation of hexoses into sucrose and starch over the course of the day.

As expected, compared to N deficiency, N fertilization stimulated glucose, fructose, and sucrose biosynthesis as indicated by the greater ear leaf concentrations in N200 and N300 treatments (Figure 2).

Coupled with the lower starch concentrations in response to N fertilization, these results indicate a noticeable change in carbon allocation, including carbon flux into starch and sucrose, as a function of plant N status [8]. Triose-phosphate/phosphate translocators located at the inner envelope membrane of chloroplasts are key regulators of carbon flux from chloroplast to cytosol [30,31]. The increased transcript abundance of *ZmTpt* in N fertilized plants suggests is consistent with greater carbon movement to the cytosol for sucrose synthesis, and reduced carbon retention in the chloroplast for starch synthesis. In parallel, the expression of the gene encoding sucrose-phosphate synthase (*ZmSps1*) was up-regulated by N fertilization. Interestingly, unlike in other plants such as duckweed [28], the expression of some of the genes related to starch biosynthesis was upregulated in response to high N fertilization, which stands in contrast to the lower starch concentrations in N-sufficient leaves (Figure 2h–j). However, the transcript abundance of the maltose exporter (*ZmMex1-like*) was elevated by N fertilization, pointing toward greater carbon mobilization from starch and export from the chloroplast. As a storage carbohydrate, starch does not demonstrate regulatory activities, but it is a major integrator in the regulation of plant growth and generally is negatively correlated to plant biomass [32]. The lower starch levels and greater mobilization under sufficient N supply suggests an enhanced starch turnover, which increases the carbon availability for export and biomass production.

Sucrose export from leaves involves symplastic transport (plasmodesmata between mesophyll cells, bundle sheath cells, and vascular parenchyma cells), and phloem loading from the apoplast [33,34]. Previously, it has been shown that both the N-deficient and N-sufficient plants had conspicuous and visually normal plasmodesmata appearances between different types of cells in leaves, indicating an open symplastic route [8]. As to the sucrose phloem loading, the process mainly involves sugar transporters including SWEETs which are responsible for the sucrose efflux from vascular parenchyma cells to the apoplast [35,36], and SUTs for the sucrose uptake from apoplastic space [37]. Of the three *Sweet13* genes examined, expression of *Sweet13a* and *Sweet13c* was responsive to N availability, with greater transcript abundance observed under sufficient N supply (Figure 3), which may indicate greater SWEET protein abundance and enhanced sucrose efflux into apoplastic space. Compared to silking, transcription of *Sweet13* genes was more responsive to N availability at 20 DAS when fast grain filling occurs, suggesting a regulatory mechanism of *Sweet13* expression that accounts for carbon demand. In addition, *ZmSut1* transcript abundance increased in response to N fertilization (Figure 3g). Taken together, the results suggest that, despite reduced photosynthetic rates under N deficiency [14], sugar export from N-deficient ear leaves is impaired even during the grain filling phase.

4.2. Nitrogen Application Influences Carbohydrate Interconversions in Developing Ears

Concentrations of the four examined carbohydrates in ears pre-silking and kernels post-silking differed considerably in response to N applications (Figure 4). Opposing trends in glucose and fructose compared to sucrose and starch concentrations at pre-silking to silking suggest that sucrose unloaded from the phloem may be cleaved to glucose and fructose in the cob prior to transport to the kernels. After moving to the kernels, the monosaccharides appear to be synthesized (transiently) into sucrose (sucrose concentration increased shortly after silking, Figure 4) and into starch. These findings are supported by the Shannon hypothesis that the ¹⁴C labeled sucrose is cleaved to fructose and glucose by acid invertase in the maternal pedicel and placento-chalazal tissue of kernels before being absorbed by the basal endosperm transfer cells in maize. Fructose and glucose are then used to form sucrose in the endosperm which in turn is used to synthesize starch in the amyloplasts [7,38–40]. Nitrogen fertilization may enhance the cleavage of sucrose to glucose and fructose in the cob prior to and at silking and the synthesis from glucose and fructose to sucrose shortly after silking (Figure 4), and thus increase kernel setting and filling. The distinct functions of these carbohydrates in processes leading to kernel set and early kernel growth, as well as a regulatory role of N status, is possibly mediated by the ratio of key amino acids such as asparagine and glutamine [5].

Shortly after silking, maize kernel glucose, fructose and sucrose concentrations exhibited a generally negative relationship with increasing N application (Figure 4a–f). However, starch accumulation in the developing kernels was positively correlated with N applications at 8 DAS and 18 DAS (Figure 4g,h). These results are consistent with studies by others that showed that increasing N supplies decreased the levels of C metabolites (sucrose and reducing sugars) in the developing kernels cultured in vitro at 20 days after pollination [16], and greater starch accumulation in developing kernels at 14 DAS in high compared to low N supply [41]. These interactions of carbon and N metabolism largely may be regulated by enzymes such as invertase, sucrose synthase and ADP-glucose pyrophosphorylase (AGPase) [16,42]. For instance, external N supply can increase AGPase activity, a limiting step in starch synthesis [16]. In any case, future studies are necessary to elucidate the molecular processes regulating carbohydrate movement, conversion and deposition in developing ears in response to various N regimes.

4.3. Source-Sink Carbon Partitioning and Grain Yield

Based on plant growth, sugar and starch dynamics, and ear development measured in this study and in the literature, we propose a conceptual model of the effect of N fertilization on source-sink carbon partitioning leading to greater grain yield (Figure 6). Although a critical value may exist (between 150 kg to 200 kg ha⁻¹ applied N in this 3-yr study) beyond which grain yield tends to decrease, N fertilization generally increases N availability and stimulates shoot growth, especially leaf area development [9,11]. The enhanced soil N availability also results in higher leaf N content, driven by increased N assimilation [18,19]. In turn, this brings about greater leaf photosynthetic capacity in N fertilized maize [9,11,12], which enhances primary carbohydrate assimilation, i.e., triose-products. The increased carbohydrate assimilation offers precursors or carbon skeletons for amino acid biosynthesis, which in turn favors photosynthesis. On the other hand, greater triose production supplies the substrates for both sucrose and starch biosynthesis [30], while N fertilization increases the triose-phosphate/phosphate translocator activity, as well as *ZmSps1*, thus promoting more carbon flux to cytosol for sucrose synthesis, and lower carbon retention in the chloroplast as starch. The increased *ZmMex1-like* expression may further accelerate transient starch turnover or mobilization, and stimulate sucrose synthesis. Upregulation of *Sweet* and *Sut1* expression would lead greater abundance of SWEET and SUT1 proteins in turn mediating enhanced sucrose export from source leaves via phloem. At the early stages of ear development, especially the two weeks bracketing silking [6], N application enhances the cleavage of sucrose to glucose and fructose in the cob prior to and at silking and the synthesis from glucose and fructose to sucrose in the kernels shortly after silking. During the fast grain filling phase, generally from 18 DAS on [5], increased conversion of sugars to starch indicates greater filling rate in N-fertilized vs. no N treated maize kernels. In turn, the greater carbon demand imposes a feedback regulation stimulating carbon assimilation and export from leaves (Figure 6).

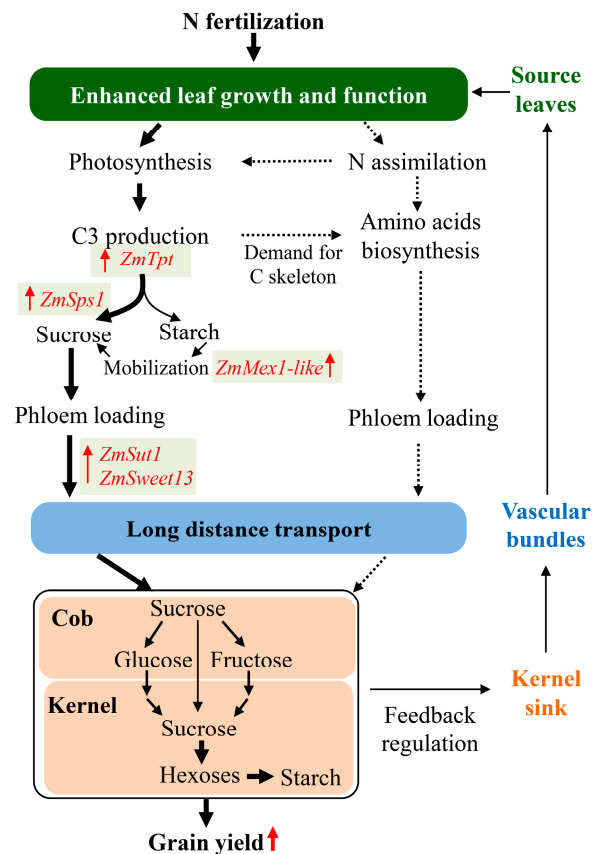


Figure 6. Schematic of a proposed metabolic pathway showing the source-sink carbon partitioning in determining the grain yield in maize under nitrogen fertilization.

5. Conclusions

In summary, greater leaf C assimilation and mobilization to the developing sink, and faster carbohydrate conversion in cobs and kernels as well as higher kernel starch accumulation around silking and during fast grain filling stages lead to the improvement of grain yield in N-fertilized maize plants. Further studies are needed to investigate the responses of key molecular players involved in sugar movement from maternal tissues to filial kernels to both low and high N availability, and their involvement in grain filling processes and yield formation.

Author Contributions: P.N., Y.P. and F.B.F. conceived and designed the experiments; P.N. and Y.P. performed the experiments, analyzed the data, and prepared the original draft. F.B.F. revised and edited the manuscript.

Funding: This research received no external funding.

Acknowledgments: The work in Northwest A&F University was supported by Natural Science Basic Research Plan in Shaanxi Province of China (No. 2018JQ3072), and the Fundamental Research Funds for the Central Universities (No. Z109021713).

Conflicts of Interest: The authors declare no conflict of interest.

References

- Ort, D.R.; Long, S.P. Limits on yields in the Corn Belt. *Science* **2014**, *344*, 484–485. [[CrossRef](#)] [[PubMed](#)]
- D Andrea, K.E.; Otegui, M.E.; Cirilo, A.G. Kernel number determination differs among maize hybrids in response to nitrogen. *Field Crop Res.* **2008**, *105*, 228–239. [[CrossRef](#)]
- Echarte, L.; Andrade, F.H.; Vega, C.R.C.; Tollenaar, M. Kernel number determination in Argentinean maize hybrids released between 1965 and 1993. *Crop Sci.* **2004**, *44*, 1654–1661. [[CrossRef](#)]
- Cantarero, M.G.; Cirilo, A.G.; Andrade, F.H. Night temperature at silking affects set in maize. *Crop Sci.* **1999**, *39*, 703–710. [[CrossRef](#)]

5. Seebauer, J.R.; Moose, S.P.; Fabbri, B.J.; Crossland, L.D.; Below, F.E. Amino acid metabolism in maize earshoots. Implications for assimilate preconditioning and nitrogen signaling. *Plant Physiol.* **2004**, *136*, 4326–4334. [[CrossRef](#)] [[PubMed](#)]
6. Hirel, B.; Le Gouis, J.; Ney, B.; Gallais, A. The challenge of improving nitrogen use efficiency in crop plants: towards a more central role for genetic variability and quantitative genetics within integrated approaches. *J. Exp. Bot.* **2007**, *58*, 2369–2387. [[CrossRef](#)] [[PubMed](#)]
7. Bihmidine, S.; Hunter, C.T.; Johns, C.E.; Koch, K.E.; Braun, D.M. Regulation of assimilate import into sink organs: update on molecular drivers of sink strength. *Front. Plant Sci.* **2013**, *4*, 177. [[CrossRef](#)]
8. Ning, P.; Yang, L.; Li, C.; Fritschi, F.B. Post-silking carbon partitioning under nitrogen deficiency revealed sink limitation of grain yield in maize. *J. Exp. Bot.* **2018**, *69*, 1707–1719. [[CrossRef](#)]
9. Ding, L.; Wang, K.J.; Jiang, G.M.; Biswas, D.K.; Xu, H.; Li, L.F.; Li, Y.H. Effects of nitrogen deficiency on photosynthetic traits of maize hybrids released in different years. *Ann. Bot.* **2005**, *96*, 925–930. [[CrossRef](#)]
10. Ciampitti, I.A.; Vyn, T.J. A comprehensive study of plant density consequences on nitrogen uptake dynamics of maize plants from vegetative to reproductive stages. *Field Crop Res.* **2011**, *121*, 2–18. [[CrossRef](#)]
11. Paponov, I.A.; Engels, C. Effect of nitrogen supply on leaf traits related to photosynthesis during grain filling in two maize genotypes with different N efficiency. *J. Plant Nutr. Soil Sci.* **2003**, *166*, 756–763. [[CrossRef](#)]
12. Uribeblanca, M.; Crafts-Brandner, S.J.; Below, F.E. Physiological N response of field-grown maize hybrids (*Zea mays* L.) with divergent yield potential and grain protein concentration. *Plant Soil* **2009**, *316*, 151–160. [[CrossRef](#)]
13. Peng, Y.; Zeng, X.; Houx, J.H.; Boardman, D.L.; Li, C.; Fritschi, F.B. Pre- and post-silking carbohydrate concentrations in maize ear-leaves and developing ears in response to nitrogen availability. *Crop Sci.* **2016**, *56*, 3218. [[CrossRef](#)]
14. Peng, Y.; Li, C.; Fritschi, F.B. Diurnal dynamics of maize leaf photosynthesis and carbohydrate concentrations in response to differential N availability. *Environ. Exp. Bot.* **2014**, *99*, 18–27. [[CrossRef](#)]
15. Peng, Y.; Li, C.; Fritschi, F.B. Apoplastic infusion of sucrose into stem internodes during female flowering does not increase grain yield in maize plants grown under nitrogen-limiting conditions. *Physiol. Plant.* **2013**, *148*, 470–480. [[CrossRef](#)]
16. Cazetta, J.O.; Seebauer, J.R.; Below, F.E. Sucrose and nitrogen supplies regulate growth of maize kernels. *Ann. Bot.* **1999**, *84*, 747–754. [[CrossRef](#)]
17. Ciampitti, I.A.; Murrell, S.T.; Camberato, J.J.; Tuinstra, M.; Xia, Y.; Friedemann, P.; Vyn, T.J. Physiological dynamics of maize nitrogen uptake and partitioning in response to plant density and nitrogen stress factors: II. Reproductive phase. *Crop Sci.* **2013**, *53*, 2588. [[CrossRef](#)]
18. Hirel, B.; Martin, A.; Tercé Laforgue, T.; Gonzalez Moro, M.B.A.; Estavillo, J.M. Physiology of maize I: A comprehensive and integrated view of nitrogen metabolism in a C4 plant. *Physiol. Plant.* **2005**, *124*, 167–177. [[CrossRef](#)]
19. Hirel, B.; Andrieu, B.; Valadier, M.H.; Renard, S.; Quilleré, I.; Chelle, M.; Pommel, B.; Fournier, C.; Drouet, J.L. Physiology of maize II: Identification of physiological markers representative of the nitrogen status of maize (*Zea mays*) leaves during grain filling. *Physiol. Plant.* **2005**, *124*, 178–188. [[CrossRef](#)]
20. Singletary, G.W.; Below, F.E. Nitrogen-induced changes in the growth and metabolism of developing maize kernels grown in vitro. *Plant Physiol.* **1990**, *92*, 160–167. [[CrossRef](#)]
21. Singletary, G.W.; Below, F.E. Growth and composition of maize kernels cultured in vitro with varying supplies of carbon and nitrogen. *Plant Physiol.* **1989**, *89*, 341–346. [[CrossRef](#)]
22. Zhao, D.; MacKown, C.T.; Starks, P.J.; Kindiger, B.K. Rapid analysis of nonstructural carbohydrate components in grass forage using microplate enzymatic assays. *Crop Sci.* **2010**, *50*, 1537. [[CrossRef](#)]
23. Lin, Y.; Zhang, C.; Lan, H.; Gao, S.; Liu, H.; Liu, J.; Cao, M.; Pan, G.; Rong, T.; Zhang, S. Validation of potential reference genes for qPCR in maize across abiotic stresses, hormone treatments, and tissue types. *PLoS ONE* **2014**, *9*, e95445. [[CrossRef](#)]
24. Pfaffl, M.W. A new mathematical model for relative quantification in real-time RT-PCR. *Nucleic Acids Res.* **2001**, *29*, e45. [[CrossRef](#)]
25. Braun, D.M.; Wang, L.; Ruan, Y.L. Understanding and manipulating sucrose phloem loading, unloading, metabolism, and signalling to enhance crop yield and food security. *J. Exp. Bot.* **2014**, *65*, 1713–1735. [[CrossRef](#)]

26. Sosso, D.; Luo, D.; Li, Q.; Sasse, J.; Yang, J.; Gendrot, G.; Suzuki, M.; Koch, K.E.; McCarty, D.R.; Chourey, P.S.; et al. Seed filling in domesticated maize and rice depends on SWEET-mediated hexose transport. *Nat. Genet.* **2015**, *47*, 1489–1493. [[CrossRef](#)]
27. Wang, L.; Lu, Q.; Wen, X.; Lu, C. Enhanced sucrose loading improves rice yield by increasing grain size. *Plant Physiol.* **2015**, 1170–2015. [[CrossRef](#)]
28. Zhao, Z.; Shi, H.; Wang, M.; Cui, L.; Zhao, H.; Zhao, Y. Effect of nitrogen and phosphorus deficiency on transcriptional regulation of genes encoding key enzymes of starch metabolism in duckweed (*Landoltia punctata*). *Plant Physiol. Biochem.* **2015**, *86*, 72–81. [[CrossRef](#)]
29. Schluter, U.; Colmsee, C.; Scholz, U.; Brautigam, A.; Weber, A.P.; Zellerhoff, N.; Bucher, M.; Fahnenstich, H.; Sonnewald, U. Adaptation of maize source leaf metabolism to stress related disturbances in carbon, nitrogen and phosphorus balance. *BMC Genom.* **2013**, *14*, 442. [[CrossRef](#)]
30. Zeeman, S.C.; Kossmann, J.; Smith, A.M. Starch: its metabolism, evolution, and biotechnological modification in plants. *Annu. Rev. Plant Biol.* **2010**, *61*, 209–234. [[CrossRef](#)]
31. Zeeman, S.C.; Smith, S.M.; Smith, A.M. The diurnal metabolism of leaf starch. *Biochem. J.* **2007**, *401*, 13–28. [[CrossRef](#)] [[PubMed](#)]
32. Sulpice, R.; Pyl, E.T.; Ishihara, H.; Trenkamp, S.; Steinfath, M.; Witucka-Wall, H.; Gibon, Y.; Usadel, B.R.; Poree, F.; Piques, M.C.O. Starch as a major integrator in the regulation of plant growth. *Proc. Natl. Acad. Sci. USA* **2009**, *106*, 10348–10353. [[CrossRef](#)] [[PubMed](#)]
33. Slewinski, T.L.; Braun, D.M. Current perspectives on the regulation of whole-plant carbohydrate partitioning. *Plant Sci.* **2010**, *178*, 341–349. [[CrossRef](#)]
34. Braun, D.M.; Slewinski, T.L. Genetic control of carbon partitioning in grasses: roles of *sucrose transporters* and *Tie-dyed* loci in phloem loading. *Plant Physiol.* **2009**, *149*, 71–81. [[CrossRef](#)] [[PubMed](#)]
35. Chen, L.; Qu, X.; Hou, B.; Sosso, D.; Osorio, S.; Fernie, A.R.; Frommer, W.B. Sucrose efflux mediated by SWEET proteins as a key step for phloem transport. *Science* **2012**, *335*, 207–211. [[CrossRef](#)] [[PubMed](#)]
36. Eom, J.; Chen, L.; Sosso, D.; Julius, B.T.; Lin, I.W.; Qu, X.; Braun, D.M.; Frommer, W.B. SWEETs, transporters for intracellular and intercellular sugar translocation. *Curr. Opin. Plant Biol.* **2015**, *25*, 53–62. [[CrossRef](#)]
37. Slewinski, T.L.; Meeley, R.; Braun, D.M. *Sucrose transporter1* functions in phloem loading in maize leaves. *J. Exp. Bot.* **2009**, *60*, 881–892. [[CrossRef](#)]
38. Felker, F.C.; Shannon, J.C. Movement of ¹⁴C-labeled assimilates into kernels of *Zea mays* L: III. An anatomical examination and microautoradiographic study of assimilate transfer. *Plant Physiol.* **1980**, *65*, 864–870. [[CrossRef](#)]
39. Shannon, J.C. Movement of ¹⁴C-labeled assimilates into kernels of *Zea mays* L: I. Pattern and rate of sugar movement. *Plant Physiol.* **1972**, *49*, 198–202. [[CrossRef](#)]
40. Shannon, J.C.; Dougherty, C.T. Movement of ¹⁴C-labeled assimilates into kernels of *Zea mays* L: II. Invertase activity of the pedicel and placento-chalazal tissues. *Plant Physiol.* **1972**, *49*, 203–206. [[CrossRef](#)]
41. Canas, R.A.; Quillere, I.; Christ, A.; Hirel, B. Nitrogen metabolism in the developing ear of maize (*Zea mays*): analysis of two lines contrasting in their mode of nitrogen management. *New Phytol.* **2009**, *184*, 340–352. [[CrossRef](#)] [[PubMed](#)]
42. Nunes-Nesi, A.; Fernie, A.R.; Stitt, M. Metabolic and signaling aspects underpinning the regulation of plant carbon nitrogen interactions. *Mol. Plant* **2010**, *3*, 973–996. [[CrossRef](#)] [[PubMed](#)]

